Slow inactivation of Na^+ current and slow cumulative spike adaptation in mouse and guinea-pig neocortical neurones in slices

Ilya A. Fleidervish, Alon Friedman and Michael J. Gutnick

Department of Physiology and Zlotowski Centre for Neuroscience, Faculty of Health Sciences, Ben-Gurion University of the Negev, Beersheva, Israel

1. Spike adaptation of neocortical pyramidal neurones was studied with sharp electrode recordings in slices of guinea-pig parietal cortex and whole-cell patch recordings of mouse somatosensory cortex. Repetitive intracellular stimulation with 1 s depolarizing pulses delivered at intervals of <5 s caused slow, cumulative adaptation of spike firing, which was not associated with a change in resting conductance, and which persisted when Co^{2+} replaced Ca^{2+} in the bathing medium.

2. Development of slow cumulative adaptation was associated with a gradual decrease in maximal rates of rise of action potentials, a slowing in the post-spike depolarization towards threshold, and a positive shift in the threshold voltage for the next spike in the train; maximal spike repolarization rates and after-hyperpolarizations were unchanged.

3. The data suggested that slow adaptation reflects use-dependent removal of Na^+ channels from the available pool by an inactivation process which is much slower than fast, Hodgkin–Huxley-type inactivation.

4. We therefore studied the properties of Na^+ channels in layer II–III mouse neocortical cells using the cell-attached configuration of the patch-in-slice technique. These had a slope conductance of 18 ± 1 pS and an extrapolated reversal potential of 127 ± 6 mV above resting potential (V_r) (mean $\pm$ S.E.M.; $n = 5$). V_r was estimated at -72 ± 3 mV ($n = 8$), based on the voltage dependence of the steady-state inactivation (h_∞) curve.

5. Slow inactivation (SI) of Na^+ channels had a mono-exponential onset with τ_{on} between 0·86 and 2·33 s ($n = 3$). Steady-state SI was half-maximal at $-43{\cdot}8$ mV and had a slope of 14·4 mV (e-fold)$^{-1}$. Recovery from a 2 s conditioning pulse was bi-exponential and voltage dependent; the slow time constant ranged between 0·45 and 2·5 s at voltages between -128 and -68 mV.

6. The experimentally determined parameters of SI were adequate to simulate slow cumulative adaptation of spike firing in a single-compartment computer model.

7. Persistent Na^+ current, which was recorded in whole-cell configuration during slow voltage ramps (35 mV s^{-1}), also underwent pronounced SI, which was apparent when the ramp was preceded by a prolonged depolarizing pulse.

In neurones, voltage-gated Na^+ channels are primarily associated with spike generation at the axon initial segment, and hence, with control of neuronal output (Hodgkin & Huxley, 1952; Moore, Stockbridge & Westerfield, 1983). Recent evidence indicates, however, that Na^+ channels are also present throughout the soma-dendritic membrane of pyramidal cells in the neocortex (Huguenard, Hamill & Prince, 1989; Amitai, Friedman, Connors & Gutnick, 1993; Stuart & Sakmann, 1994) and the hippocampus (Magee & Johnston, 1995; Spruston, Schiller, Stuart & Sakmann, 1995), suggesting that they also play a significant role in synaptic integration within the dendritic tree. At the initial segment, high Na^+ channel density assures a large safety factor for spike generation, even though a substantial fraction of the channels may be functionally unavailable due to inactivation (Moore *et al.* 1983; Spruston *et al.* 1995). By contrast, relatively small changes in Na^+ channel availability might significantly influence function of the soma-dendritic membrane, where channel density is probably much lower (Huguenard *et al.* 1989; Stuart & Sakmann, 1994).

Fast Na^+ channel inactivation, represented as the h parameter in the Hodgkin–Huxley equations, is characterized by rapid onset upon depolarization and rapid recovery following a brief hyperpolarizing interval (Hodgkin & Huxley, 1952). In addition, a slowly developing and much longer lasting suppression of Na^+ currents is observed when squid axons (Rudy, 1978) or other neural (Rudy, 1981; Howe & Ritchie, 1992; Ruben, Starkus & Rayner, 1992) and muscle (Reuter, 1968; Ruff, Simoncini & Stuhmer, 1988; Zilberter, Motin, Sokolova, Papin & Khodorov, 1991) preparations are subjected to prolonged periods of depolarization. The kinetics of 'slow inactivation' (SI) have not been described for central neurones. In preparations where it has been studied, the time constant of recovery from SI is in the order of seconds, suggesting that entrance of channels into this inactivated state might be an important, activity-dependent determinant of neuronal excitability, especially under pathological conditions of intense discharge such as epilepsy. In the present study, we have examined SI in neocortical neurones. We report that prolonged discharge causes neocortical pyramidal cells to undergo slow, cumulative adaptation of spike firing, and that a very long time is required for recovery. Using cell-attached 'patch-in-slice' recordings, we show that Na^+ channels in these neurones do undergo SI, and that the kinetics of this process are appropriate to account for the slow adaptation.

METHODS

Slice preparation and maintenance

Experiments were performed in 400 μm thick coronal slices of somatosensory cortex of 8- to 16-week-old guinea-pigs or 1- to 4-week-old CD1 mice. Procedures for preparation and maintenance of slices were similar to those described previously for this laboratory (Friedman & Gutnick, 1989). Animals of either sex were deeply anaesthetized with Nembutal (60 mg kg^{-1}), killed by decapitation, and their brains rapidly removed and placed in cold (6 °C), oxygenated (95% O_2–5% CO_2) artificial cerebrospinal fluid (ACSF). Coronal slices from a region corresponding to the primary somatosensory cortex were cut 400 mm thick on a vibratome (Vibroslice), and placed in holding bottles containing ACSF at room temperature; they were transferred to a recording chamber after more than 1 h of incubation.

Sharp electrode recording

Slices of guinea-pig neocortex were maintained in a fluid–gas interface chamber at a temperature thermostatically held at 36 ± 0·5 °C. Recordings were made with glass microelectrodes that were filled with 4 M potassium acetate and had impedances of 60–80 MΩ. Data were collected with a Neuro Data amplifier, stored on video tape using a Neuro-Corder (Neuro Data), digitized off-line and analysed using pCLAMP 5.5 (Axon Instruments).

Patch-clamp recording

Slices of mouse neocortex were maintained in a submersion chamber and a 'blind' patch-clamp technique (Blanton, Lo Turco & Kriegstein, 1989) was used to record either Na^+ channel currents or transmembrane potential and currents. Single Na^+ channels were recorded in cell-attached configuration and whole-cell current was recorded in whole-cell configuration using an Axopatch-1D amplifier (Axon Instruments). Transmembrane potential was recorded in whole-cell configuration using an Axoclamp-2A amplifier in bridge mode. Patch pipettes were manufactured from thick-walled borosilicate glass capillaries (1·5 mm o.d.), coated to within 100 μm of the tip with Sylgard (Dow Corning); electrode resistance was 1·5–3·5 MΩ. All cell-attached recordings were made at room temperature (22–24 °C); whole-cell recordings were made at 32 °C.

Command voltage protocols were generated and single-channel data were acquired on-line with an Axolab 1100 A/D interface. Data were low-pass filtered at 2 kHz (−3 dB, 4-pole Bessel filter) and sampled at 10–20 kHz digitalization frequency. Before data acquisition, capacitive and leak currents were reduced using the built-in circuits of the amplifier. Null traces for digital subtraction of remaining capacitive and leak current components were produced by stepping from a depolarized membrane potential, at which all Na^+ channels in the patch were inactivated. For whole-cell current clamp recording, data were low-pass filtered at 10 kHz (−3 dB, single-pole Bessel filter), stored on video tape and digitized off-line at up to 20 kHz.

Recording from cell-attached patches usually lasted between 20 and 60 min; in some cases it was possible to record for up to 2 h without significant changes in seal resistance or resting potential (V_r). Stability of V_r was periodically tested by measuring the voltage dependence of Na^+ channel availability (h_∞). In most patches, K^+ channel activity was also recorded at voltages between −40 and +120 mV relative to V_r. K^+ channel activity was not recorded when 1 mM 4-aminopyridine (4-AP) and 10 mM tetraethylammonium (TEA) were present in the pipette solution.

For whole-cell recordings of persistent Na^+ current ($I_{Na,P}$), care was taken to maintain membrane access resistance as low as possible (usually 3–4 MΩ; never >10 MΩ); series resistance was 80% compensated.

Solutions

ACSF contained (mM): NaCl, 124; KCl, 3; $CaCl_2$, 2; $MgSO_4$, 2; NaH_2PO_4, 1·25; $NaHCO_3$, 26; glucose, 10 (pH 7·3). The pipette solution for cell-attached experiments contained (mM): NaCl, 130; KCl, 3; $CaCl_2$, 2; $MgCl_2$, 2; glucose, 10; TEA-Cl, 10; 4-AP, 1; Hepes (sodium salt), 10 (pH 7·3). The pipette solution for whole-cell current clamp experiments contained: KCl, 135; K-EGTA, 0–10; $MgCl_2$, 2; Hepes (potassium salt), 10 (pH 7·25). The pipette solution for whole-cell persistent sodium current recording contained: CsCl, 135; NaCl, 4; Cs-EGTA, 0–10; $MgCl_2$, 2; Hepes (caesium salt), 10 (pH 7·25).

Data analysis

Data averaging, digital subtraction of null traces and current peak detection were made using pCLAMP 5.5 software. Data were fitted by exponential and Boltzmann curves using a Levenberg–Marquardt fitting routine.

Computer simulations

Numerical computations were made using the NEURON simulation program (Hines, 1989), implemented on a SUN SPARC-IPC workstation, as previously described in detail (Reuveni, Friedman, Amitai & Gutnick, 1993). For simplicity, the modelled cell was taken as a single isopotential compartment. The passive membrane properties were membrane resistance (R_m) = 125 000 Ω cm^2, membrane capacitance (C_m) = 1 μF cm^{-2}, and input resistance (R_{input}) = 300 MΩ; resting potential was set to −70 mV, which is close to the mean value we obtained for

cortical neurones in the present study (see Results). Na^+ and K^+ channels were introduced using the Hodgkin–Huxley formalism. In adjusting the kinetics of simulated Na^+ current to match experimental observations made at room temperature, a temperature coefficient (Q_{10}) of 3 was assumed (Hodgkin & Huxley, 1952; Rudy, 1978). Maximal Na^+ and K^+ conductances and K^+ current kinetics were adjusted to fit action potential parameters and firing patterns of RS neocortical neurones (Connors & Gutnick, 1990).

The Na^+ current was given by the equation:

$$I_{Na} = G_{Na} m^3 hs(V_m - E_{Na}),$$

where V_m is membrane potential, the equilibrium potential for Na^+ (E_{Na}) = +50 mV and Na^+ conductance (G_{Na}) = 10 mS cm^{-2}. The activation variable m was described by:

$$\alpha = 0{\cdot}091(V_m + 40)/(1 - \exp(-(V_m + 40)/5)),$$

$$\beta = -0{\cdot}062(V_m + 40)/(1 - \exp(V_m + 40)/5)).$$

The fast inactivation variable, h, was defined by:

$$\alpha = 0{\cdot}06 \exp((-55 - V_m)/15),$$

$$\beta = 6{\cdot}01 (\exp(17 - V_m)/21) + 1).$$

Slow inactivation was modelled by adding the variable, s, which was defined such that α and β would fit the experimentally determined time course and voltage dependence shown in Figs 7, 8 and 9. In order to simplify the model, we assumed that s varied between 0 and 1, and that $Q_{10} = 3$ (Hodgkin & Huxley, 1952; Rudy, 1978). s was given by:

$$\alpha = 0{\cdot}001 \exp((-85 - V_m)/30),$$

$$\beta = 0{\cdot}0034(\exp(-17 - V_m)/10) + 1).$$

A delayed rectifier K^+ current was introduced:

$$I_K = G_K n^4 (V_m - E_K),$$

$$\alpha = 0{\cdot}034(V_m + 45)/(1 - \exp(-(V_m + 45)/5)),$$

$$\beta = 0{\cdot}54 \exp(-75 - V_m)/40)),$$

where the equilibrium potential for K^+ (E_K) = −90 mV.

The slow K^+ current had a similar voltage activation curve to I_K, with time constants ten times slower.

RESULTS

Slow, cumulative adaptation of spike firing

Current clamp recordings were made with sharp electrodes from forty-three neurones in layer II–III of adult guinea-pig somatosensory cortex. All cells had resting potentials more negative than −70 mV and overshooting action potentials. All were identified as 'regular spiking' (RS) neurones on the basis of their responses to current injection (Connors, Gutnick & Prince, 1982; Connors & Gutnick, 1990). In a later series of experiments, voltage recordings were made from ten neurones in the same layers in slices of mouse SM1 cortex using patch clamp in the whole-cell configuration. Although input resistances under these conditions were generally more than an order of magnitude higher than in the sharp electrode recordings, the basic phenomenology of spike frequency adaptation was essentially the same.

When depolarized by single, prolonged, suprathreshold current pulses, RS neurones typically showed spike frequency adaptation (Fig. 1). With repetitive stimulation at intervals briefer than 5 s, the frequency adaptation became more and more prominent from pulse to pulse; in >50% of the neurones ($n = 25$), this cumulative adaptation resulted in failure of spike generation midway during the later pulses of the stimulus train. Thus, in the representative neurone of Fig. 1*A*, repetitive stimulation with 1 s pulses delivered every 1·6 s caused a gradual slowing of the firing frequency from pulse to pulse, such that firing failed towards the end of the 4th response (Fig. 1*A a*). In Fig. 1*A b*, after a 60 s recovery period, the same neurone was stimulated every 2·5 s; at this slower frequency, onset of the cumulative adaptation was more gradual and spike failure did not appear until the 17th stimulus. When spike generation failed, it was generally replaced by a subthreshold oscillation of membrane potential reminiscent of the 'damped oscillations' recorded in squid axons (see Guttman & Barnhill, 1970).

Ca^{2+}-dependent K^+ currents have been implicated as an underlying mechanism of firing adaptation in hippocampal neurones (Madison & Nicoll, 1984) and neocortical neurones (Schwindt, Spain, Foehring, Stafstrom, Chubb & Crill, 1988; Friedman & Gutnick, 1989). The slowly developing adaptation, however, was not associated with a change in resting conductance, as measured by hyperpolarizing current pulses between stimuli (not shown). We tested for a role of Ca^{2+} influx by omitting Ca^{2+} from the bathing solution and adding 5 mM Co^{2+} in its place. Although this manipulation did result in some increase in firing rate (see Friedman & Gutnick, 1989), Co^{2+} did not prevent fast frequency adaptation during the course of individual stimuli, nor did it prevent gradual development of cumulative adaptation during repetitive stimulation (Fig. 1*C*).

The above experiment showed that slow adaptation was not caused by influx of Ca^{2+} and consequent activation of a Ca^{2+}-dependent current. Figure 2 shows that many of the features of the phenomenon were consistent with a gradual, use-dependent decrease in Na^+ channel availability. The neurone illustrated in this figure was stimulated with 800 ms pulses delivered every 2·5 s. The graphs of Fig. 2*A* plot the instantaneous firing frequency as a function of time during the pulse for the 1st, 5th and 9th stimuli in the train. During the first stimulus there was an initial phase of rapid adaptation which lasted 50–100 ms and was followed by a phase of slow adaptation. As the stimulus train progressed, a third adaptation phase appeared with increasing prominence late in the course of each pulse. Figure 2*B* plots the maximal depolarization rates of all the action potentials during the 1st, 9th and 13th stimuli in the train, and Fig. 2*D* plots the maximal spike repolarization rates during the 1st, 5th, 9th and 13th stimuli. It can be seen that the depolarization rate, which is most sensitive to

the available Na^+ conductance (Hodgkin & Huxley, 1952; i.e. to the availability of Na^+ channels), decreased as the stimulus train progressed. By contrast, the repolarization rate, which is primarily sensitive to changes in magnitude of repolarizing K^+ currents (Hodgkin & Huxley, 1952), was unchanged throughout the train. A reasonable explanation for the slow cumulative adaptation, therefore, is a progressive decrease in the availability of Na^+ channels. This conclusion is supported by examination of the traces in Fig. 2*C*, which shows superimposed individual spikes recorded 500 ms after the onsets of the 1st, 9th and 15th stimuli; these have been lined up at the peak without changing the voltage axis. Note that as the train proceeded, the post-spike depolarizing trajectory towards threshold became slower, and there was a positive shift in the threshold voltage for the next action potential. There was little or no change in the spike after-hyperpolarization (AHP), however, suggesting that there was no build up of K^+ current.

The kinetics of voltage-dependent fast inactivation are too rapid to contribute to the slow, use-dependent adaptation. Fast inactivation can account for the rapid fall in action potential rate-of-rise at the onset of each pulse (Fig. 2*B*). As illustrated by Fig. 1*B*, however, the fraction of Na^+ channels that are in the fast inactivated state can be reactivated following a hyperpolarizing pulse that is far too brief to restore the neurone from slow adaptation (see below). When the cell in Fig. 1*B* was repetitively stimulated at 0·33 Hz, by the 18th stimulus action potential generation failed midway through each pulse. At this time, a 30 ms hyperpolarization released a burst of three spikes with decreasing amplitudes, but it did not affect the slow adapted state, which required at least 5 s at resting potential for full recovery.

The above evidence suggested that although slow adaptation does reflect use-dependent removal of Na^+ channels from the available pool, it is not a manifestation of fast inactivation. In the next series of experiments, we characterized slow Na^+ channel inactivation in neocortical neurones, in order to determine whether its parameters are appropriate to account for the phenomenon of slow adaptation of spike firing.

Na^+ channel currents

The cell-attached patch clamp configuration was used to record single Na^+ channels from forty-eight superficial neurones in layers II and III of mouse neocortical slices. In

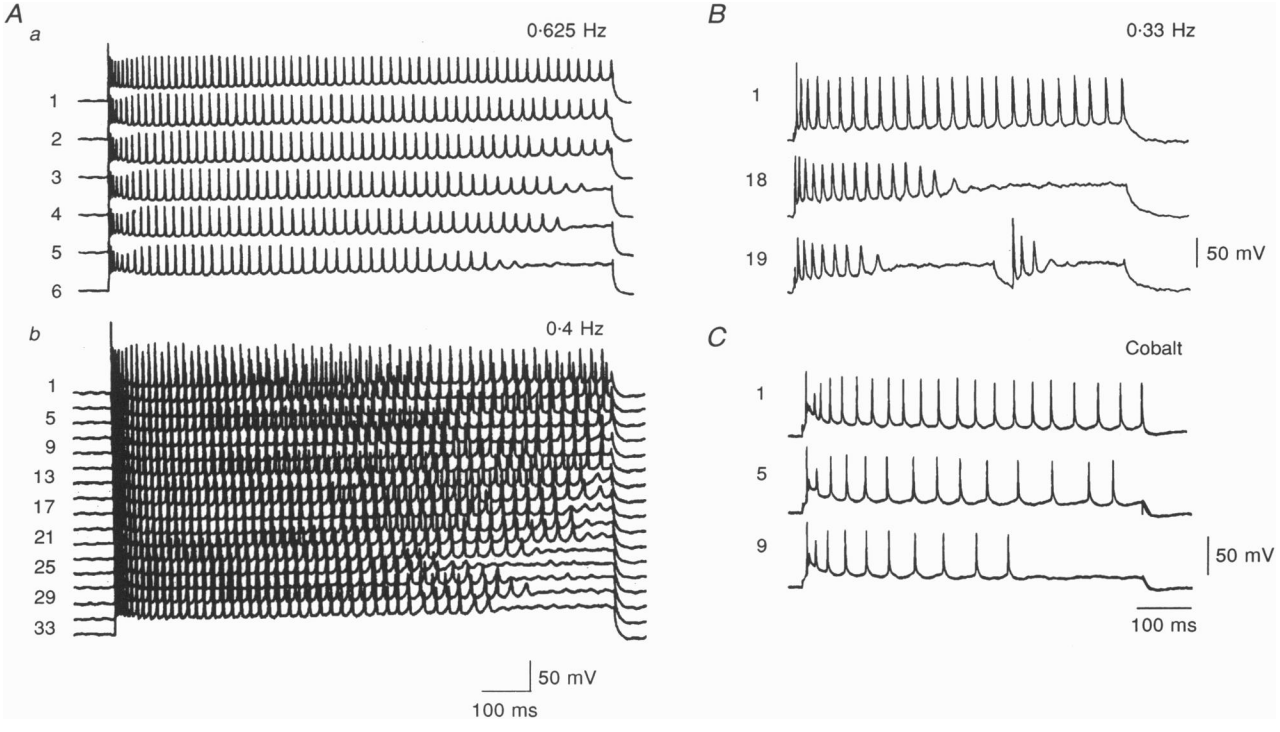

Figure 1. Repetitive stimulation elicits slow cumulative adaptation

Sharp electrode recording from a layer II–III neurone in guinea-pig neocortical slice during 1 s depolarizing current pulses. *A a*, stimulation every 1·6 s causes a gradual decrease in spike frequency from pulse to pulse; by the 4th stimulus, spike firing failed late in the pulse. *A b*, when the same neurone was stimulated every 2·5 s, failure to generate action potentials did not appear until the 17th stimulus. *B*, in a different neurone, after slow cumulative adaptation has been induced by 18 repetitive stimuli delivered every 3 s, a brief (30 ms) hyperpolarizing pulse elicits only a transient recovery of spike firing. *C*, in a different neurone, slow cumulative adaptation persists in a bathing medium that contains nominal 0 Ca^{2+} and 5 mM Co^{2+}. Stimulus number indicated to the left of each trace.

all cases, Na^+ channels were activated when the potential of the patch was held at a level 20–40 mV negative to the neurone's resting membrane potential (V_r) and a suprathreshold depolarizing test pulse was applied. Na^+ channels were identified as such on the basis of polarity and the characteristic voltage-dependent kinetics (Fig. 3*A*). Although bath-applied TTX does not block Na^+ channels recorded in the cell-attached configuration, bath-applied lidocaine is effective under these conditions (Alzheimer, Schwindt & Crill, 1993). Bath application of 50 μM lidocaine completely and reversibly abolished the channel activity ($n = 3$). The conductance of single Na^+ channels was similar to that previously reported for neocortical neurones (Huguenard, Hamill & Prince, 1988; Alzheimer *et al.* 1993). Slope conductance, as determined from a linear fit to the *I–V* curve of the single open-channel in the range of $V_r + 20$ to $V_r + 70$ mV, was 18 ± 1 pS; the extrapolated reversal potential was $V_r + 127 \pm 6$ mV (mean ± S.E.M.; $n = 5$). Assuming that V_r is near −70 mV (see below), we estimate from the Nernst equation an internal Na^+ activity of about 15 mM.

Na^+ channel openings first appeared at test pulse amplitudes between +10 and +25 mV (18 ± 3 mV, $n = 5$; Fig. 3). As shown in the representative traces of Fig. 3*A*, progressively increasing test potential amplitude caused openings to cluster at the beginning of the pulse and late openings to become rarer. Occasionally, however, bursts of openings lasted throughout the duration of the depolarization (Fig. 3*A*).

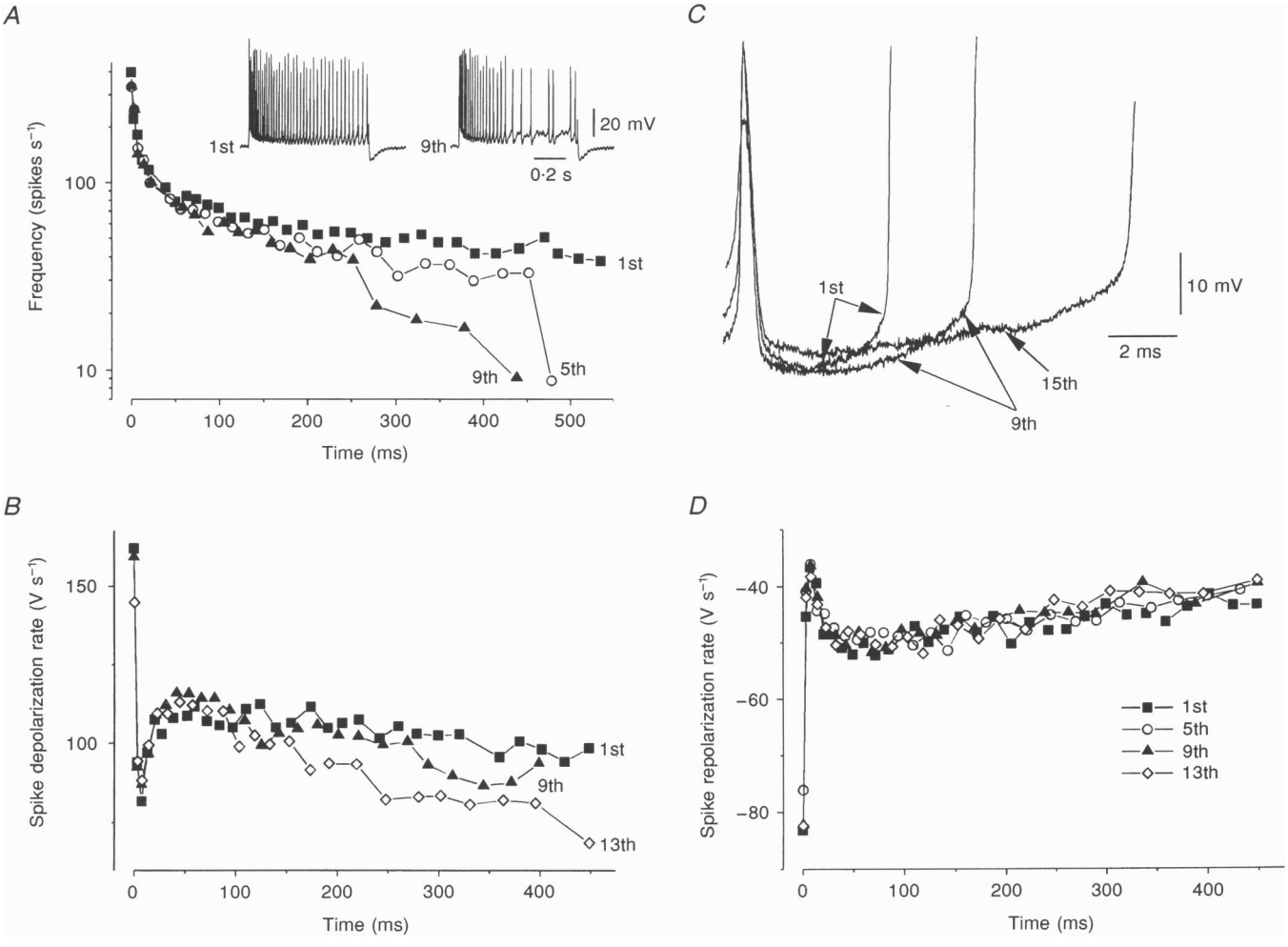

Figure 2. Change in spike characteristics during repetitive activation with 800 ms depolarizing pulses delivered every 2·5 s

A, pulse to pulse decrease in spike frequency. Inset, responses to 1st and 9th stimuli. *B*, biphasic change in maximal velocity of the rising phase of each action potential (dV/dt_{max}) during the 1st, 9th and 13th stimuli in the train. Note the gradual slowing in rate of rise from stimulus to stimulus. *C*, action potentials from the latter part of the 1st, 9th and 15th stimulus pulses have been superimposed, to show: (1) that there is almost no change in AHP amplitude, (2) that there is a gradual slowing of post-spike depolarization towards the threshold for the next spike, and (3) that there is a gradual positive shift in the threshold voltage. *D*, maximal rates of repolarization for each action potential in the 1st, 5th, 9th and 13th stimulus pulses do not change.

In the cell-attached configuration, the actual membrane voltage is a sum of the command voltage imposed by the experimenter, and the resting potential, which is unknown. Unless otherwise noted, we refer to the command voltage in the following text.

All patches contained multiple channels, as indicated by the appearance of overlapping opening events. We strove for patches containing fifteen or more channels in order to obtain relatively smooth averages with only thirty to fifty sweeps (Fig. 3*B*). Since the vast majority of the patches contained less than eight channels (Huguenard *et al.* 1988; Stuart & Sakmann, 1994), only about one in ten was used in the present study. In order to minimize fluctuations in peak amplitude from one average current to another with this small number of sweeps we generally used test voltages more positive than +50 mV, so that open probability would be nearly maximal.

Analysis of *I–V* curves for peak averaged Na^+ currents (Fig. 3*C*) revealed a maximum at between +50 and +65 mV ($n = 5$). Figure 3*D* shows the conductance transform of these data, obtained by dividing the peak current by the driving force (as estimated from the single open-channel current–voltage relationship). Data points were fitted with the following Boltzmann-type equation:

$$G_{Na}/G_{Na,max} = 1/[1 + \exp((V_{½} - V_{test})/k)],$$

where $G_{Na,max}$ – the maximum Na^+ conductance – is the average value of all peak Na^+ conductances within 2% of the largest conductance, $V_{½}$ is the test potential at which G_{Na} is half-maximal, and k is the slope of the fitted curve at $V_{½}$. In the figure, $G_{Na,max}$ was normalized to a value of one. For the five cells in which activation was studied in great detail, $V_{½}$ was +31 to +45 mV, and k was 6·1 to 8·8 mV (e-fold)$^{-1}$.

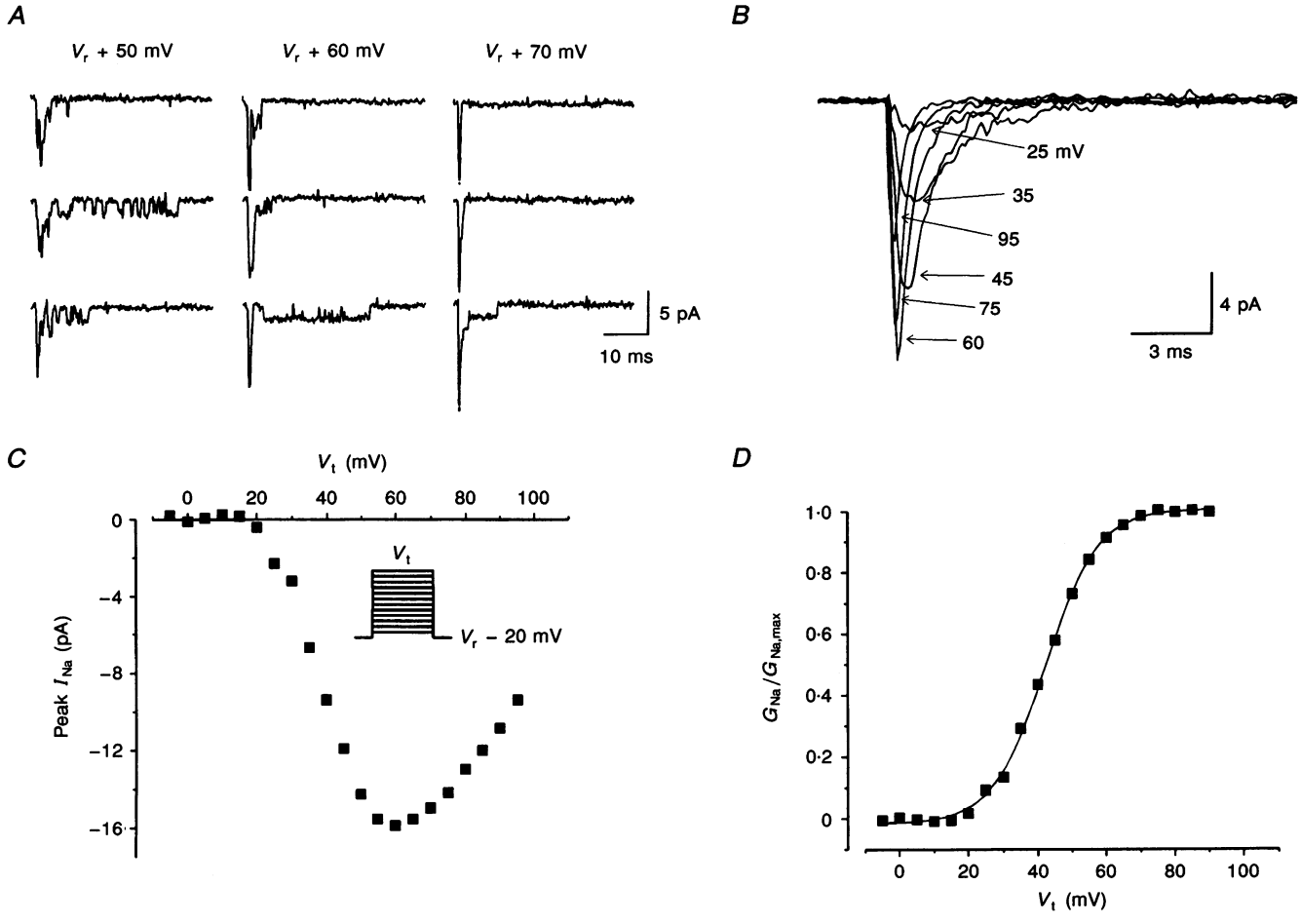

Figure 3. Characteristics of Na^+ channel currents in cell-attached patches of layer II–III neurones of mouse neocortical slices

A, representative currents during 40 ms depolarizing pulses to specified test potentials from a holding potential of V_r – 40 mV. Note the occasional bursts of late openings, which presumably underlie the persistent Na^+ current ($I_{Na,P}$). Channel currents were filtered at 2 kHz (–3 dB) and digitized at 10 kHz. *B*, ensemble Na^+ currents from a different neurone obtained by averaging 40 sweeps at each test potential. *C*, *I–V* relationship of peak Na^+ currents from same neurone as in *B*. Currents were elicited with voltage steps that incremented by 5 mV, starting from V_r – 5 mV (see protocol in inset). *D*, activation curve obtained by conductance transform of the data in *C*. Continuous line is the best fit by a Boltzmann equation ($V_{½} = V_r + 42$ mV; $k = 7·7$ mV (e-fold)$^{-1}$).

Figure 4*A* shows the protocol used to plot a classic steady-state fast inactivation (h_∞) curve. Following a 50 ms conditioning pulse to various voltages from the holding potential of −40 mV, the membrane patch was stepped to the test voltage of +70 mV. To construct the graph of Fig. 4*A*, the peak of the average test current (I_{test}) following each conditioning voltage step (V_{cond}) was normalized relative to the maximal current (I_{max}). Because I_{max} fluctuated, maximal current was taken as the average of all peak currents that fell within 2% of the largest current recorded (see Howe & Ritchie, 1992). Results were fitted by a Boltzmann-type equation of the form:

$$I_{test}/I_{max} = 1/[1 + \exp((V_{cond} - V_{½})/k)].$$

Figure 4*B* shows the h_∞ curves for eight different neurones. $V_{½}$ varied in the range of −1 to +10 mV and k varied from 7·2 to 10·5 mV (e-fold)$^{-1}$. Using whole-cell recordings from isolated neocortical neurones, Huguenard *et al.* (1988) measured an average $V_{½}$ of −68 mV and k of 8·8 mV (e-fold)$^{-1}$. If we assume that the voltage dependence of Na^+ channel steady-state inactivation is the same for neocortical neurones in the slice, we can estimate the resting potential of the cell as $V_r = -68 - V_{½}$. Thus, for the eight neurones illustrated in Fig. 4*B*, V_r varied between −67 and −78 mV (−72 ± 3 mV).

Slow inactivation of Na^+ channels

Prolonged depolarization caused a gradual decrease in Na^+ conductance that was consistent with a reduction in channel availability with very slow onset and recovery. This suggests that, in addition to the fast inactivation state, h, there exists a slow inactivation state, s, whose entrance and exit rate constants are slower by orders of magnitude.

The inset of Fig. 5 shows the voltage protocol used to determine the time course of onset of slow inactivation; it consisted of a control test pulse (V_1), followed by a conditioning prepulse (V_{cond}) of variable duration (t_{cond}) and a subsequent test pulse (V_2), followed by a return to the holding potential of −20 mV for 5 s. A 40 ms delay at −20 mV was imposed between the end of V_{cond} and the onset of V_2 to allow full recovery from fast inactivation. All depolarizing pulses were to +50 mV, and t_{cond} was varied systematically between 40 ms and 6 s. The superimposed traces in Fig. 5 show the Na^+ currents recorded before (I_1) and after (I_2) conditioning pulses that were 0·2 s (left traces) and 2 s (right traces) in duration. It can be seen that while a decrease in peak I_{Na} was only barely detectable following the briefer V_{cond}, I_2 was significantly depressed by the prolonged prepulse, which drove a sizeable fraction of the Na^+ channels into a slow inactivating state. The graph of

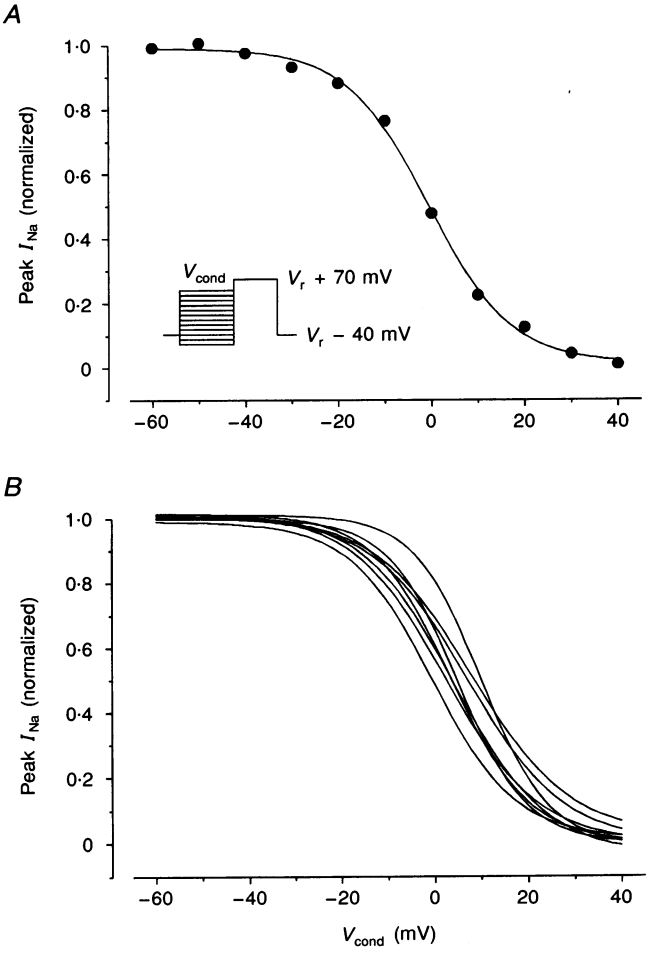

Figure 4. Steady-state inactivation (h_∞) of I_{Na} in neocortical neurones

A, h_∞ curve for a single, representative cell. Membrane patches were held at V_r − 40 mV. Test currents were elicited with voltage steps to V_r + 70 mV following 50 ms inactivating prepulses (V_{cond}) which started at V_r − 60 mV and incremented by 10 mV (see protocol in inset). ●, peak Na^+ currents (normalized to maximal I_{Na}). Continuous curve is the best fit by a Boltzmann equation ($V_{½} = V_r - 1$ mV, $k = 8·9$ mV (e-fold)$^{-1}$). *B*, best-fit h_∞ curves for 8 different neurones. Note that they have similar steepness but differ as to $V_{½}$. This is probably due to differences in V_r.

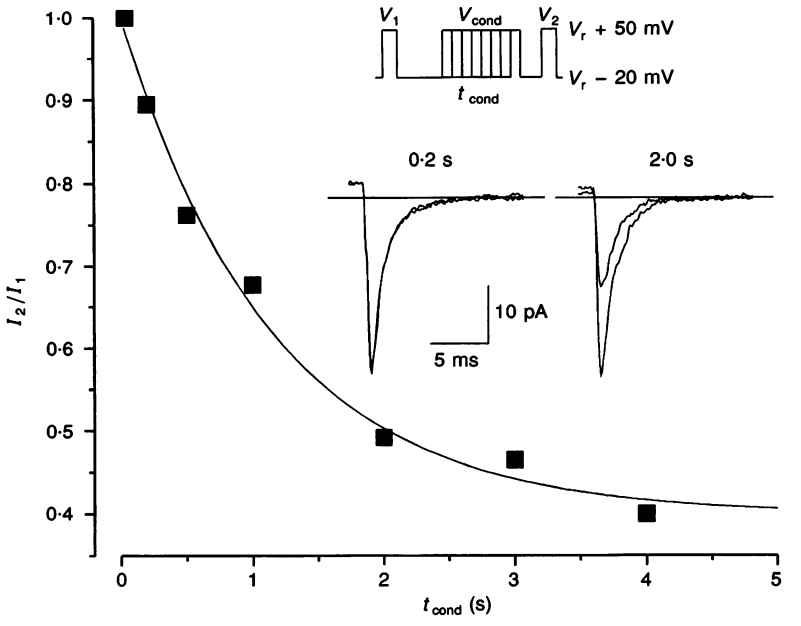

Figure 5. Onset of SI of I_{Na}

Top inset, stimulus protocol, consisting of an initial test pulse (V_1), a conditioning prepulse (V_{cond}) of variable duration (t_{cond}), a 40 ms interval (to permit full recovery from fast inactivation), and a 2nd test pulse (V_2). Bottom inset: Superimposed I_{Na} traces before and after 0·2 s (left) and 2·0 s (right) conditioning prepulses. Graph, filled squares plot the ratio between peak I_{Na} elicited by second and first pulses, as a function of conditioning prepulse duration. Continuous curve, mono-exponential best fit; for this cell, $s_\infty = 0{\cdot}42$ and $\tau_{on} = 0{\cdot}86$ s.

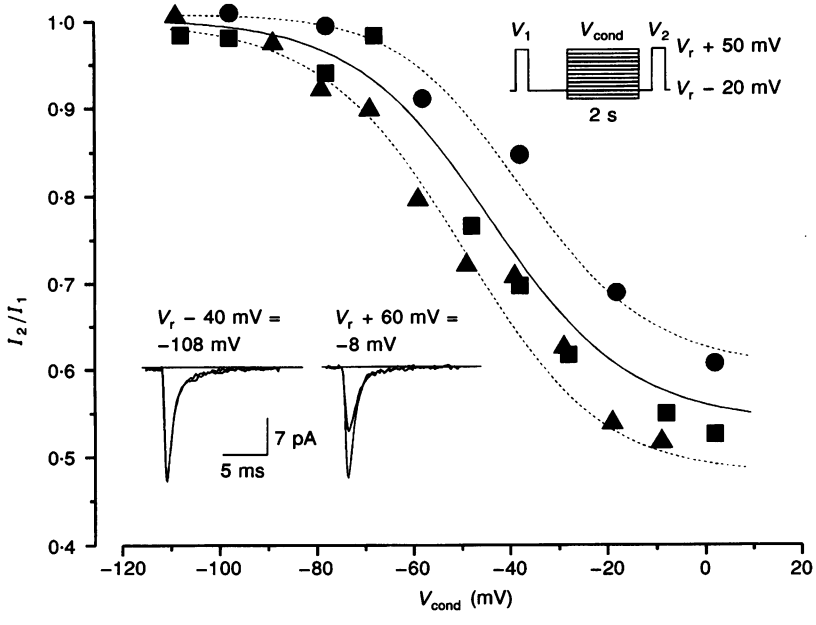

Figure 6. Voltage dependence of SI of I_{Na}

Top inset, same stimulus protocol as in Fig. 7, except that the duration of V_{cond} was held constant at 2 s, and its amplitude was systematically varied between $V_r - 40$ mV and $V_r + 80$ mV. Bottom inset, superimposed I_{Na} traces before and after conditioning prepulses to $(V_r - 40) = -108$ mV (left) and $(V_r + 60) = -8$ mV (right). Graph, for 3 different neurones (●, ■ and ▲), I_2/I_1 ratios plotted as a function of voltage of V_{cond} (expressed in absolute values, based on estimation of V_r from the voltage dependence of the h_∞ curve). Each curve was fit by a Boltzman equation; plotted are the mean (continuous curve) and S.D. (dashed curve) of the fits.

Fig. 5 plots the s variable, i.e. the ratio I_2/I_1, as a function of t_{cond}. The continuous curve shows the best fit of the data by the exponential equation:

$$s = s_\infty + (1 - s_\infty)\exp(-t_{cond}/\tau_{on}),$$

where s_∞ is the fraction of Na^+ channels that are not slow-inactivated at steady state, and τ_{on} is the time constant of slow inactivation onset. In three such experiments, s_∞ ranged from 0·25 to 0·42 and τ_{on} ranged from 0·86 to 2·33 s.

The inset of Fig. 6 shows the protocol used to determine the voltage dependence of slow inactivation. Na^+ channel availability was tested 40 ms after the end of a prolonged prepulse, which was systematically varied between −40 and +70 mV. The duration of the conditioning prepulse was fixed at 2 s in order to limit the time required for each experiment; 90 s was required for a single trial such as the one shown in Fig. 6, and acquisition of thirty trials took at least 45 min of stable recording. The traces in Fig. 6 show superimposed Na^+ currents before and after a prepulse to $V_{cond} = -40$ mV (left) and +60 mV (right). When added to V_r, as estimated from the h_∞ curve (see above), they correspond to membrane voltages of $V_{cond} + V_r = -108$ and −8 mV, respectively. The graph in Fig. 8 plots the ratio of the peak currents before and after the 2 s pulse (I_2/I_1), as a function of $V_{cond} + V_r$. Results of each experiment were fit by a Boltzmann-type equation of the form:

$$s = (s_{max} - s_{min})/[1 + \exp((V_{cond} - V_{½})/k)],$$

where s_{max} and s_{min} are, respectively, maximal and minimal Na^+ channel availabilities after the 2 s conditioning pulses, $V_{½}$ is the prepulse potential at which 'steady-state' slow inactivation was half-maximal, and k is the slope of the fitted curve at $V_{½}$. The continuous curve and the dashed curves in Fig. 6 show the mean and S.D. of three fitted curves ($s_{max} = 1·00$, $s_{min} = 0·54$, $V_{½} = -43·8$ mV and $k = 14·4$ mV (e-fold)$^{-1}$).

Figure 7 illustrates experiments in five additional neurones to determine the time course and voltage dependence of recovery from slow inactivation. The inset in Fig. 7*A* shows the protocol used. Slow inactivation was induced by a 2 s conditioning depolarization, the patch was held for varying

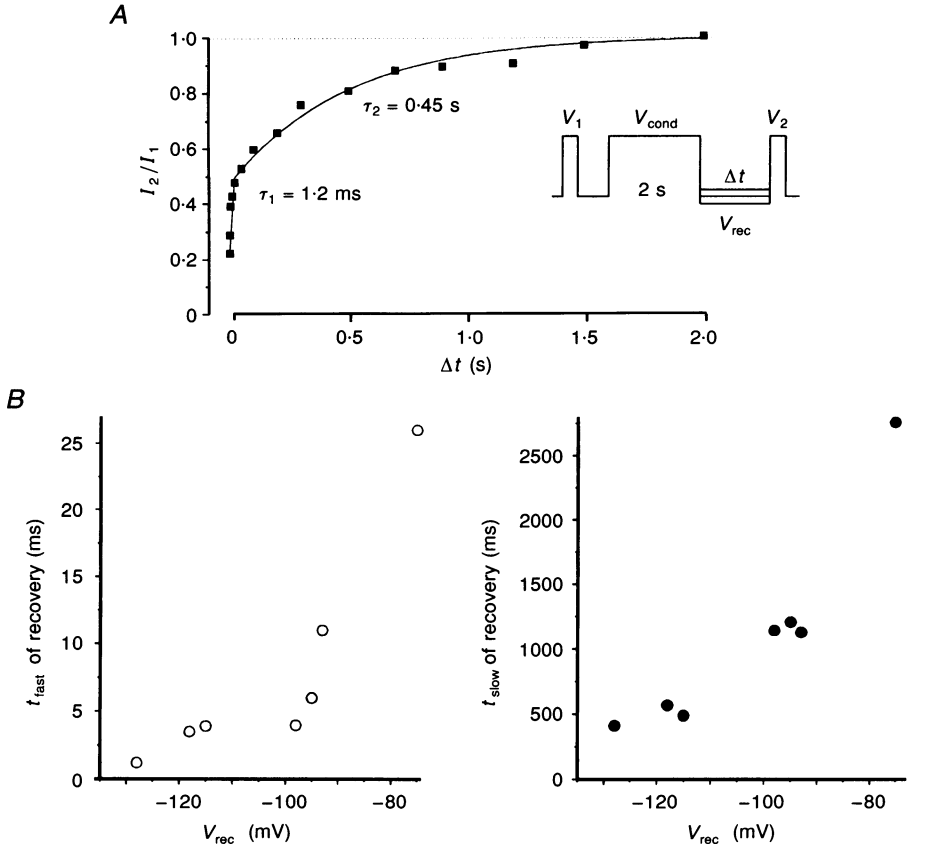

Figure 7. Time course and voltage dependence of recovery of I_{Na} from SI

A, recovery after 2 s conditioning pulse to $V_r + 70$ mV has a bi-exponential time course. At $V_r - 60 = -128$ mV, about 50% of the channels (those presumably in the fast inactivation state) recovered with a time constant of 1·2 ms, and the remaining channels recovered with a time constant of 0·45 s. *B*, fast and slow recovery time constants at different membrane potentials, obtained from 5 different neurones. Voltages given in absolute values, based on estimates of V_r from the voltage dependence of the h_∞ curve, as in Fig. 6.

periods at a given membrane potential, and it was then stepped to a test voltage (V_2) to assess the fraction of Na^+ current available for activation (I_2/I_1). At all potentials examined, recovery followed a bi-exponential time course, and was well fitted by the equation:

$$I_2/I_1 = h_\infty + I_f \exp(-t/\tau_f) + I_s \exp(-t/\tau_s).$$

The second exponential was readily distinguished from the first because it was about two orders of magnitude slower. Thus, in the cell illustrated in Fig. 7*A*, when recovery voltage was $V_r + (-60)$ mV (i.e. -128 mV), about half the Na^+ channels recovered with a time constant of 1·2 ms (these presumably were those recovering from the fast inactivation state); the remaining channels recovered with a time constant of 0·45 s. From the graphs of Fig. 7*B*, which show the voltage dependence of τ_f and τ_s for five neurones, it is evident that both time constants were extremely slow when recovery voltage was near the resting potential.

Computer simulation of slow, cumulative adaptation

In order to evaluate whether slow inactivation of Na^+ channels can account for the observed slow cumulative adaptation of RS neurones, current-clamp experiments such as those in Fig. 1 were simulated in a single compartment computer model. In Fig. 8, a 1 s depolarizing pulse was delivered to the model neurone every 2 s. An s variable, which was defined such that it fitted the experimentally observed voltage and time dependence of the slow inactivation process, was introduced in a Hodgkin–Huxley-type equation for Na^+ current (see Methods). In the absence of slow inactivation (i.e. s held constant at 1) there was no slow cumulative adaptation; the model cell followed the low frequency repetitive stimulus with only slight accommodation, the extent of which depended on activation of the slow K^+ conductance (Fig. 8, left). When a realistic s variable was included, however, the results of the simulation (Fig. 8, right) were similar to the experimental data of Fig. 1.

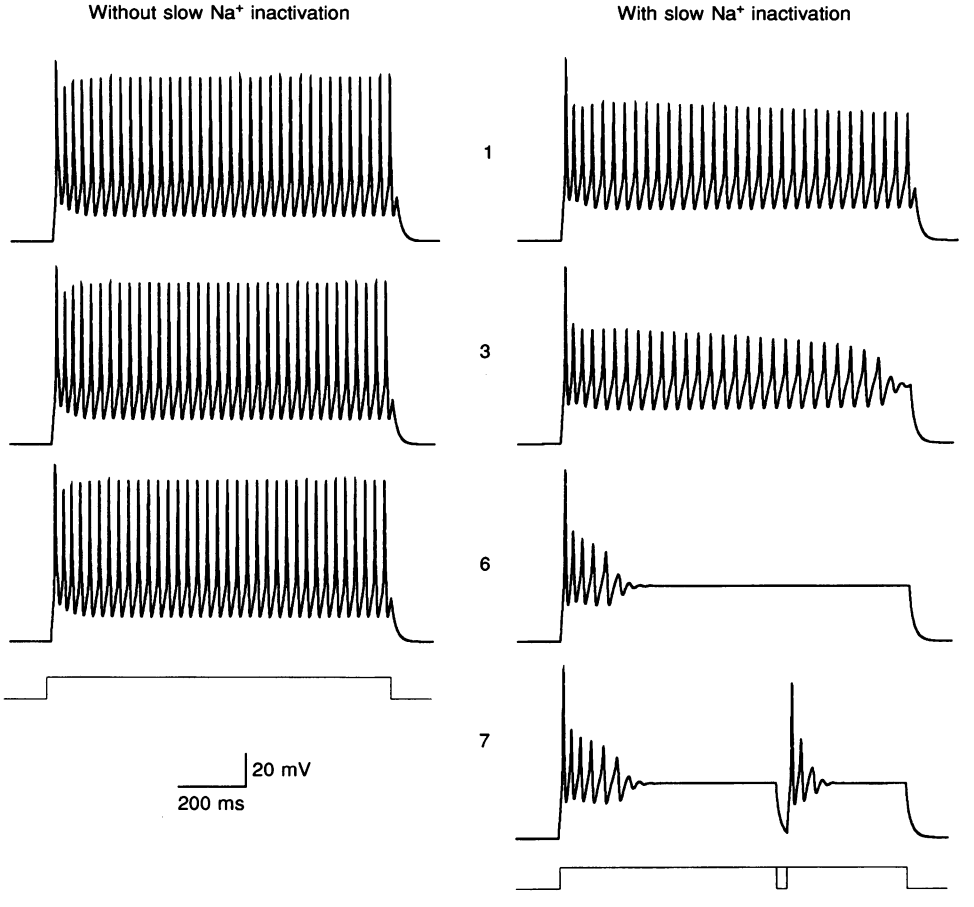

Figure 8. Computer simulation of neuronal firing in a single-compartment model during repetitive stimulation with 1 s depolarizing pulses delivered every 2 s

Left, when I_{Na} was limited to m^3h kinetics, the firing response did not change throughout the course of the train. Right, upon addition of a SI variable, s, based on experimentally determined parameters, the model cell underwent typical slow cumulative adaptation which was similar to the experimental observations (cf. Fig. 1).

Slow inactivation of $I_{Na,P}$

Neocortical neurones possess a prominent persistent Na^+ current ($I_{Na,P}$), which does not undergo fast inactivation and which is activated at more negative potentials than is the fast I_{Na} (Connors *et al.* 1982; Stafstrom, Schwindt & Crill, 1982; Stafstrom, Schwindt, Chubb & Crill, 1985; Brown, Schwindt & Crill, 1994). Because $I_{Na,P}$ may play a prominent role in determining spike threshold (Connors *et al.* 1982; Stafstrom *et al.* 1982) and determining active conduction properties of dendrites, it was important to determine whether this current too is susceptible to slow inactivation following prolonged depolarization or repetitive firing.

In fifteen mouse layer V neurones recorded in whole-cell configuration at 32 °C, $I_{Na,P}$ was revealed as the TTX-sensitive current component during slow (35 mV s^{-1}) voltage ramps from −70 to 0 mV. For these experiments, patch pipettes contained Cs^+ as the main cation to block K^+ currents, and 200 μM Cd^{2+} was added to the bath to block Ca^{2+} currents. Figure 9 shows the instantaneous *I–V* curves generated under these conditions before and after addition of TTX to the bath. $I_{Na,P}$ began to activate at about −60 mV, and reached a peak at between −35 and −25 mV. At membrane potentials more positive than −25 mV, $I_{Na,P}$ was obscured by an outward current, which has been previously described as a non-specific cationic current (Alzheimer, 1994). This was the only current component that remained unblocked when the pipette solution contained 50–500 μM QX-314 ($n = 5$, not shown) or 10^{-8}–10^{-6} M TTX was applied to the bath (Fig. 9). Figure 10 illustrates the effects of preceding the ramps by conditioning prepulses to +20 mV. It can be seen that whereas conditioning steps briefer than 0·1 s did not affect $I_{Na,P}$, 1–10 s prepulses caused significant, duration-dependent depression of the persistent current.

DISCUSSION

The major finding of this study is that Na^+ currents in neocortical neurones undergo slow inactivation, and that the kinetics of this process are appropriate to explain slow, cumulative adaptation of spike firing.

Slow adaptation of spike firing

Although neocortical neurones are heterogeneous in terms of spike adaptation characteristics, all 'regular spiking' cells undergo some degree of fast adaptation, as evidenced by a gradual increase in interspike intervals during a spike train (Connors *et al.* 1982; Connors & Gutnick, 1990). We here describe an additional adaptation process which is very much slower and is cumulative over the course of

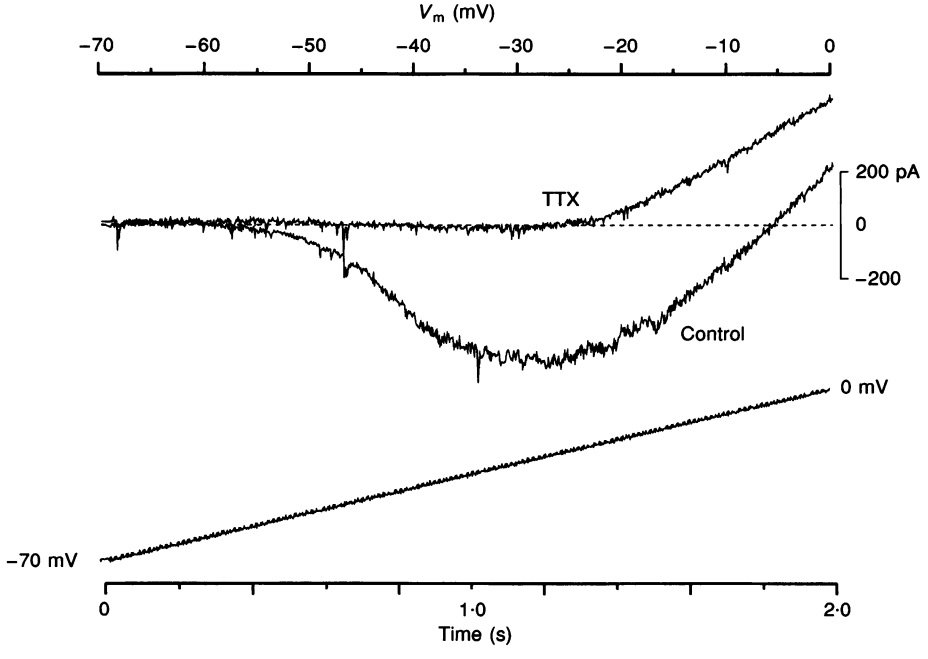

Figure 9. Persistent Na^+ current in a mouse neocortical neurone

Instantaneous *I–V* curves were obtained in whole-cell configuration during a slow (35 mV s^{-1}) depolarizing ramp from −70 to 0 mV. Access resistance, 4 MΩ; leakage subtracted; 32 °C. $I_{Na,P}$, which was identified as the TTX-sensitive component of membrane current, first activated at about −60 mV, and reached a peak at between −35 and −25 mV. At membrane potentials positive to −25 mV, $I_{Na,P}$ overlapped with an outward, TTX-resistant current. (For recordings in Figs 9 and 10, ACSF contained 200 μM Cd^{2+} and Cs^+ was the main monovalent cation in the recording pipettes.)

many seconds. Neocortical neurones possess a Ca^{2+}-dependent K^+ conductance (Schwindt *et al.* 1988; Friedman & Gutnick, 1989), and gradual build up of such a conductance has been implicated in slow spike adaptation in hippocampal neurones (Madison & Nicoll, 1984). This cannot account for the phenomenon described here, however, since slow adaptation persisted in the presence of Ca^{2+} channel blockers (Fig. 1*C*). Neocortical neurones also possess a Na^+-dependent K^+ conductance (Schwindt *et al.* 1988); however, because the slow adaptation was not associated with a shift in resting potential or resting conductance in the intervals between spike trains, we conclude that it was not caused by this K^+ current either. The progressive changes in spike characteristics during development of the slow adaptation (Fig. 2) strongly suggest gradual removal of Na^+ channels from the available pool. The phenomenon is too slow to be due to fast inactivation of Na^+ channels, which has a recovery time constant at resting potential that is no greater than 25 ms at room temperature (Huguenard *et al.* 1988; Ruben *et al.* 1992; Huang, 1993; see Fig. 7). This leaves slow inactivation – a distinct (Rudy, 1978; Patlak, 1991; Ruben *et al.* 1992) voltage sensitive process which has been described for a wide variety of preparations, including skeletal muscle (Ruff *et al.* 1988), squid giant axon (Rudy, 1978), *Myxicola* giant axon (Rudy, 1981), cardiac myocyte (Reuter, 1968; Zilberter *et al.* 1991), neuroblastoma cell (Quandt, 1988) and glial cell (Howe & Ritchie, 1992).

Although evidence of SI was previously noted in isolated suprachiasmatic neurones (Huang, 1993), ours is the first description of its characteristics in a central neurone. We were particularly interested in determining onset and offset time constants of SI in neocortical cells, since these values may differ somewhat in different preparations (see Table 3 in Howe & Ritchie, 1992) and they are critical for evaluating whether SI can explain the observed slow spike adaptation. For example, Rudy (1981) showed that in *Myxicola* axons, onset of SI was extremely rapid (time constant measured in milliseconds) and only the recovery time constant was slow (measured in seconds); while these parameters accounted well for an inability of that axon to sustain prolonged repetitive firing (Rudy, 1981), they are not appropriate to explain slow adaptation of neocortical neurones. We show that entry to the SI state and recovery from it are both slow in neocortex. The computer simulations of Fig. 8 indicate that these SI kinetics are sufficient to account for the spike firing behaviour.

Na^+ current kinetics

The characteristics of Na^+ currents in this study were basically the same as previously reported for central neurones. Most such studies have entailed whole-cell recording from isolated neurones (Huguenard *et al.* 1988; Sah, Gibb & Gage, 1988; Cummins, Xia & Haddad, 1994). The whole-cell configuration cannot be used to study Na^+ current kinetics in the morphologically complex pyramidal cells of the intact neocortical slice, however, because the current is too large, too fast and too spatially distributed to permit voltage control (Muller & Lux, 1993). In the cell-attached configuration, the actual membrane voltage is the sum of the voltage command and V_r, which is unknown. In

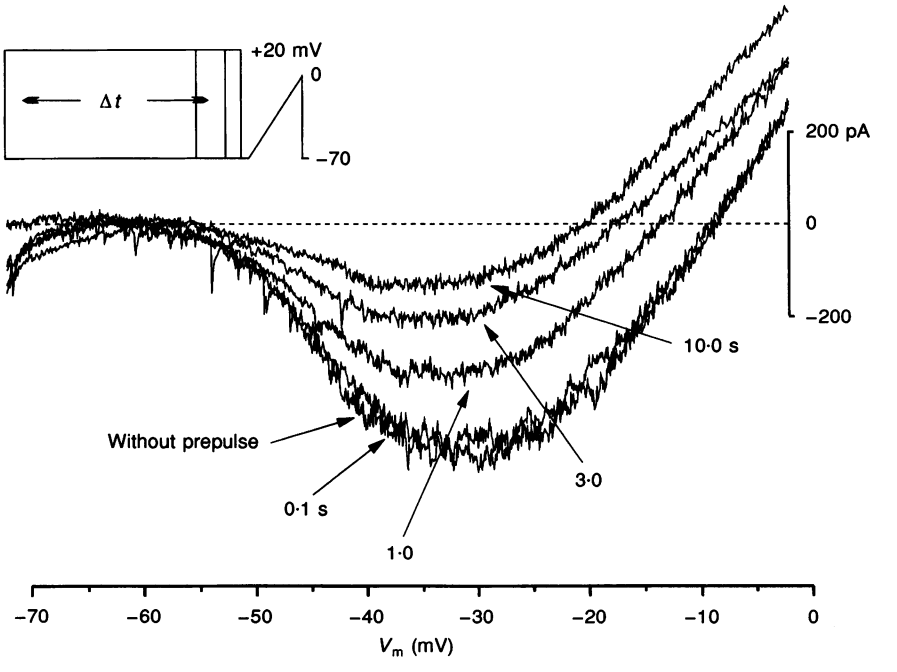

Figure 10. $I_{Na,P}$ underwent SI when the voltage ramp (as in Fig. 9) was preceded by a conditioning step to +20 mV

Note that as the duration of the conditioning pulse increased, the magnitude of $I_{Na,P}$ decreased accordingly.

view of the general uniformity of neural Na^+ channel kinetics in different preparations (Patlak, 1991), we estimated V_r by assuming that the midpoint of the h_∞ curve in our cells was the same as that experimentally determined for isolated neocortical cells by Huguenard *et al.* (1988). This approach may offer some advantages in illuminating the relationship between channel kinetics and neuronal function. True V_r cannot be measured using recording techniques that disrupt the membrane, because these influence resting potential by causing a leak and/or by dialysing the cell. In the present study, we estimate the resting potential of neocortical neurones at -72 ± 3 mV. This value is about midway between that reported for sharp electrode studies (Connors *et al.* 1982; Friedman & Gutnick, 1989) and that reported for whole-cell patch-clamp recordings (Stuart & Sakmann, 1994). Whatever the accuracy of our estimate, our data do give precise, functionally relevant information as to the availability of Na^+ channels at V_r and the voltage deviation from rest necessary to reach activation threshold.

Slow inactivation of Na^+ channels

In virtually all cells in which it has been tested, the time course of recovery of Na^+ current from inactivation induced by prolonged (100 ms to 10 s) depolarizing prepulses may be described as a sum of three exponentials (Zilberter *et al.* 1991; Howe & Ritchie, 1992; for review see Patlak, 1991). We have focused here on the fastest, which is recovery from classical inactivation as described by Hodgkin & Huxley (1952), and on the slowest, which corresponds to SI. Although we also saw evidence of the intermediate time course of recovery, we have not considered it here, nor have we sought evidence of ultra-slow inactivation (Ruff *et al.* 1988). Our study has not addressed the molecular basis of SI. Evidence from other studies indicates that fast and slow inactivation are separate processes mediated by different molecular mechanisms (Ruben *et al.* 1992) which are pharmacologically distinct (Rudy, 1978). The kinetics of SI have been reported to vary widely in different preparations (see Table 3 in Howe & Ritchie, 1992); in general, the values for neocortical neurones are similar to those reported for Na^+ channels in cardiac myocytes (Zilberter *et al.* 1991), glial cells (Howe & Ritchie, 1992) and Crayfish axons (Ruben *et al.* 1992).

One functionally important parameter of SI which varies from study to study is the midpoint of the s_∞ curve. We found it to be at -45 mV, which is about 25 mV more depolarized than that of the h_∞ curve. Similar values were reported by others (Zilberter *et al.* 1991; Howe & Ritchie, 1992). Some workers, however, have reported values more hyperpolarized than the midpoint of steady-state fast inactivation (Belluzzi & Sacchi, 1986; Ruff *et al.* 1988; Ruben *et al.* 1992). The reason for this difference is not clear.

It is noteworthy that even with 6 s prepulses, which is more than three times greater than τ_{on}, only 70% of the Na^+ channels were in the SI state. Similar results have been reported for cardiac myocytes (Zilberter *et al.* 1991) and for glial cells (Howe & Ritchie, 1992). Our data are insufficient to suggest a kinetic scheme that would explain this. It is possible that some Na^+ channels never enter the SI state, or that, as with fast inactivation (Patlak & Ortiz, 1985), there exists a distinct mode of Na^+ channel kinetics which fail to enter the SI state.

Slow inactivation of $I_{Na,P}$

Neocortical neurones, like many other central neurones (see Taylor, 1993), posses a prominent $I_{Na,P}$ which apparently reflects temporary gating of the same Na^+ channel into a non-inactivating mode (Alzheimer *et al.* 1993; Brown *et al.* 1994). Here, we present evidence that with prolonged depolarization, $I_{Na,P}$ does undergo slow inactivation. This finding, which correlates well with evidence from other preparations that SI persists after fast inactivation has been removed pharmacologically (Rudy, 1978), is consistent with the generally accepted hypothesis that the molecular mechanisms underlying fast and slow inactivation are distinct (see above). It will be interesting to determine whether the kinetics of SI are the same for $I_{Na,P}$ as for the transient current.

Because $I_{Na,P}$ activates at a more negative voltage than does the transient current (Brown *et al.* 1994), it should have an important functional role in setting spike threshold and determining the repetitive firing characteristics of the neurone (Connors *et al.* 1982; Stafstrom *et al.* 1982). In the present experiments, slow inactivation of $I_{Na,P}$ is probably responsible for the gradual increase in spike threshold and prolongation of inter-spike voltage trajectory that characterized the development of slow cumulative spike adaptation (Fig. 2). Although $I_{Na,P}$ has not been explicitly measured in dendrites, neocortical dendrites do possess Na^+ channels (Huguenard *et al.* 1989; Amitai *et al.* 1993; Stuart & Sakmann, 1994), and it seems likely that here, as elsewhere, they occasionally enter a non-inactivating mode. Subthreshold activation of dendritic $I_{Na,P}$ may play an important role both in 'boosting' distal synaptic inputs (Schwindt & Crill, 1995) and promoting active 'back propagation' of somatic action potentials into the dendrites (Stuart & Sakmann, 1994). Consequently, use-dependent slow inactivation of $I_{Na,P}$ may be an important dynamic factor in determining the functional integrative properties of the dendrites (see below).

Functional significance of slow Na^+ inactivation in neocortical neurones

At steady state, the fraction of Na^+ channels available to respond to depolarization is governed by two independent processes: fast inactivation and slow inactivation. Because the voltage sensitivities and kinetics of the two differ greatly in the neocortical neurone, each will have a different functional impact. At resting potential, 50% of the Na^+ channels abide in the fast inactivated state (Fig. 4). The h_∞ curve is quite steep at this voltage, however, and

recovery is on the order of milliseconds. Thus, only a brief hyperpolarizing interval is required before the channel can again be opened by subsequent depolarization; interaction between voltage-gated and synaptic currents can rapidly reprime the Na^+ channels that have accumulated in this state, making them immediately available for participation in brisk neuronal responses to small voltage changes.

By contrast, recovery from SI at physiologically realistic membrane potentials is in the order of seconds, and once Na^+ channels enter this state, prolonged hyperpolarization is required to reprime them. The midpoint of the s_∞ curve is relatively depolarized (−45 mV), the slope of the curve is not steep, and entrance to the SI state is quite slow. Accordingly, only 2–10% of the Na^+ channels abide in this state at V_r and even large depolarizations will have little lasting effect unless they are very prolonged. Rudy (1981) proposed that the long recovery time from slow inactivation may limit the frequency at which impulses pass in *Myxicola* axons, and Ruff *et al.* (1988) suggested a similar functional role for SI in rat muscle fibres. We show here that in neocortical neurones, repetitive, high frequency discharge can induce sufficient SI to limit the ability to fire. Functionally, such persistent high frequency firing might only be encountered under pathological conditions such as ictal epileptic discharge. Indeed, based on their experiments in neuroblastoma cells, Quandt (1988) proposed that the anticonvulsant effect of diphenylhydantoin may be due to enhancement of slow inactivation of Na^+ channels.

The kinetics of SI suggest that it may also play a dynamic role in determining excitability of neocortical neurones under 'normal' conditions. Unit recordings from neocortical cells in behaving animals reveal low spontaneous firing rates; according to Abeles (1991), the mean rate is about 5 Hz and more than half the cells fire at less than 2 Hz. Although entrance to the SI state is slow, recovery is slower. Each action potential should therefore leave in its wake a prolonged period of slightly decreased Na^+ channel availability. A simple calculation shows that at $V_r = -70$ mV, a spontaneous firing rate of 1 Hz may increase the fraction of Na^+ channels in the SI state by about 10%, and that 10 Hz activity might remove up to 30% from the available pool. Less than 10 s would be required to achieve these steady state levels, and the recent 'spontaneous' firing history of the neurone could thus be a significant factor in determining its excitability at any moment.

Of course, the functional consequences of removing a large fraction of the Na^+ channels from the available pool depends on the 'safety factor' for spike initiation and propagation, which, in turn, depends on cable properties and on Na^+ channel density. Although, as noted above, Na^+ channels are present throughout the soma-dendritic membrane of neocortical pyramidal cells, physiological evidence indicates they are not evenly distributed. Thus, even when spikes are elicited by an intradendritic current injection, they always originate somewhere near the soma (Amitai *et al.* 1993; Stuart & Sakmann, 1994). This finding has been interpreted as an indication that Na^+ channel density in the dendrites is considerably lower than in the initial segment (Stuart & Sakmann, 1994; Mainen, Joerges, Huguenard & Sejnowski, 1995). A relatively low dendritic Na^+ channel density, combined with the dendritic cable properties, can account for the finding that backpropagation is decremental rather than 'all-or-none' in nature (Spruston *et al.* 1995; Mainen *et al.* 1995). Spruston *et al.* (1995) recently reported that back propagation of spikes in CA1 hippocampal neurones is frequency dependent as well. They recorded simultaneously at the soma and at the dendrite during somatic spike trains, and showed that active propagation of spikes into the dendrites gradually failed as the train progressed. Inactivation of Na^+ channels was one of the possible explanations offered to account for this phenomenon. Indeed, the time course and voltage dependence of activity-dependent dendritic spike failure (Spruston *et al.* 1995) are in good agreement with the kinetics of slow inactivation we report here.

To summarize this point: back propagation of action potentials into dendrites seems to be critically dependent on the availability of dendritic Na^+ channels. We propose that even under conditions of relatively low frequency 'spontaneous' firing, slow inactivation of Na^+ channels, while insufficient to compromise neuronal output from the channel-rich initial segment, may modify active dendritic propagation. This may be a mechanism whereby factors that control the firing history of neocortical neurones thereby control integration in their dendrites.

Abeles, M. (1991). *Corticonics: Neural Circuits of the Cerebral Cortex.* Cambridge University Press, Cambridge.

Alzheimer, C. (1994). A novel voltage-dependent cation current in rat neocortical neurones. *Journal of Physiology* **479**, 199–205.

Alzheimer, C., Schwindt, P. C. & Crill, W. E. (1993). Modal gating of Na^+ channels as a mechanism of persistent Na^+ current in pyramidal neurons from rat and cat sensorimotor cortex. *Journal of Neuroscience* **13**, 660–673.

Amitai, Y., Friedman, A., Connors, B. W. & Gutnick, M. J. (1993). Regenerative activity in apical dendrites of pyramidal cells in neocortex. *Cerebral Cortex* **3**, 26–38.

Belluzzi, O. & Sacchi, O. (1986). A quantitative description of the sodium current in the rat sympathetic neurone. *Journal of Physiology* **380**, 275–291.

Blanton, M. G., Lo Turco, J. J. & Kriegstein, A. R. (1989). Whole cell recording from neurons in slices of reptilian and mammalian cerebral cortex. *Journal of Neuroscience Methods* **30**, 203–210.

Brown, A. M., Schwindt, P. C. & Crill, W. E. (1994). Different voltage dependence of transient and persistent Na^+ currents is compatible with modal-gating hypothesis for sodium channels. *Journal of Neurophysiology* **71**, 2562–2565.

CONNORS, B. W. & GUTNICK, M. J. (1990). Intrinsic firing patterns of diverse neocortical neurons. *Trends in Neurosciences* **13**, 99–104.

CONNORS, B. W., GUTNICK, M. J. & PRINCE, D. A. (1982). Electrophysiological properties of neocortical neurons in vitro. *Journal of Neurophysiology* **48**, 1302–1320.

CUMMINS, T. R., XIA, Y. & HADDAD, G. G. (1994). Functional properties of rat and human neocortical voltage-sensitive sodium currents. *Journal of Neurophysiology* **71**, 1052–1064.

FRIEDMAN, A. & GUTNICK, M. J. (1989). Intracellular calcium and control of burst generation in neurons of guinea-pig neocortex *in vitro*. *European Journal of Neuroscience* **1**, 374–381.

GUTTMAN, R. & BARNHILL, R. (1970). Oscillation and repetitive firing in squid axons. Comparison of experiments with computations. *Journal of General Physiology* **55**, 104–118.

HINES, M. (1989). A program for simulation of nerve equation with branching geometries. *International Journal of Biomedical Computation* **24**, 55–68.

HODGKIN, A. L. & HUXLEY, A. F. (1952). A quantitative description of membrane current and its application to conduction and excitation in nerve. *Journal of Physiology* **117**, 500–544.

HOWE, J. R. & RITCHIE, J. M. (1992). Multiple kinetic components of sodium channel inactivation in rabbit Schwann cells. *Journal of Physiology* **455**, 529–566.

HUANG, R. C. (1993). Sodium and calcium currents in acutely dissociated neurons from rat suprachiasmatic nucleus. *Journal of Neurophysiology* **70**, 1692–1703.

HUGUENARD, J. R., HAMILL, O. P. & PRINCE, D. A. (1988). Developmental changes in Na^+ conductances in rat neocortical neurons: appearance of a slowly inactivating component. *Journal of Neurophysiology* **59**, 778–795.

HUGUENARD, J. R., HAMILL, O. P. & PRINCE, D. A. (1989). Sodium channels in dendrites of rat cortical pyramidal neurons. *Proceedings of the National Academy of Sciences of the USA* **86**, 2473–2477.

MADISON, D. V. & NICOLL, R. A. (1984). Control of the repetitive discharge of rat CA1 pyramidal neurones *in vitro*. *Journal of Physiology* **354**, 319–331.

MAGEE, J. C. & JOHNSTON, D. (1995). Characterization of single voltage-gated Na^+ and Ca^{2+} channels in apical dendrites of rat CA1 pyramidal neurons. *Journal of Physiology* **487**, 67–90.

MAINEN, Z. F., JOERGES, J., HUGUENARD, J. R. & SEJNOWSKI, T. J. (1995). A model of spike initiation in neocortical pyramidal neurons. *Neuron* **15**, 1427–1439.

MOORE, J. W., STOCKBRIDGE, N. & WESTERFIELD, M. (1983). On the site of impulse initiation in a neurone. *Journal of Physiology* **336**, 301–311.

MULLER, W. & LUX, H. D. (1993). Analysis of voltage-dependent membrane currents in spatially extended neurons from point-clamp data. *Journal of Neurophysiology* **69**, 241–247.

PATLAK, J. (1991). Molecular kinetics of voltage-dependent Na^+ channels. *Physiological Reviews* **71**, 1047–1080.

PATLAK, J. B. & ORTIZ, M. (1985). Slow currents through single sodium channels of the adult rat heart. *Journal of General Physiology* **86**, 89–104.

QUANDT, F. N. (1988). Modification of slow inactivation of single sodium channels by phenytoin in neuroblastoma cells. *Molecular Pharmacology* **34**, 557–565.

REUTER, H. (1968). Slow inactivation of currents in cardiac Purkinje fibres. *Journal of Physiology* **197**, 233–253.

REUVENI, I., FRIEDMAN, A., AMITAI, Y. & GUTNICK, M. J. (1993). Stepwise repolarization from Ca plateaus in neocortical pyramidal cells: evidence for nonhomogeneous distribution of HVA Ca channels in dendrites. *Journal of Neuroscience* **13**, 4609–4621.

RUBEN, P. C., STARKUS, J. G. & RAYNER, M. D. (1992). Steady-state availability of sodium channels. Interactions between activation and slow inactivation. *Biophysical Journal* **61**, 941–955.

RUDY, B. (1978). Slow inactivation of the sodium conductance in squid giant axons. Pronase resistance. *Journal of Physiology* **283**, 1–21.

RUDY, B. (1981). Inactivation in *Myxicola* giant axons responsible for slow and accumulative adaptation phenomena. *Journal of Physiology* **312**, 531–549.

RUFF, R. L., SIMONCINI, L. & STUHMER, W. (1988). Slow sodium channel inactivation in mammalian muscle: a possible role in regulating excitability. *Muscle and Nerve* **11**, 502–510.

SAH, P., GIBB, A. J. & GAGE, P. W. (1988). The sodium current underlying action potentials in guinea pig hippocampal CA1 neurons. *Journal of General Physiology* **91**, 373–398.

SCHWINDT, P. C., SPAIN, W. J., FOEHRING, R. C., STAFSTROM, C. E., CHUBB, M. C. & CRILL, W. E. (1988). Multiple potassium conductances and their functions in neurons from cat sensorimotor cortex in vitro. *Journal of Neurophysiology* **59**, 424–449.

SCHWINDT, P. C. & CRILL, W. E. (1995). Amplification of synaptic current by persistent sodium conductance in apical dendrite of neocortical neurons. *Journal of Neurophysiology* **74**, 2220–2224.

SPRUSTON, N., SCHILLER, Y., STUART, G. & SAKMANN, B. (1995). Activity-dependent action potential invasion and calcium influx into hippocampal CA1 dendrites. *Science* **268**, 297–300.

STAFSTROM, C. E., SCHWINDT, P. C., CHUBB, M. C. & CRILL, W. E. (1985). Properties of persistent sodium conductance and calcium conductance of layer V neurons from cat sensorimotor cortex in vitro. *Journal of Neurophysiology* **53**, 153–170.

STAFSTROM, C. E., SCHWINDT, P. C. & CRILL, W. E. (1982). Negative slope conductance due to a persistent subthreshold sodium current in cat neocortical neurons *in vitro*. *Brain Research* **236**, 221–226.

STUART, G. J. & SAKMANN, B. (1994). Active propagation of somatic action potentials into neocortical pyramidal cell dendrites. *Nature* **367**, 69–72.

TAYLOR, C. P. (1993). Na^+ currents that fail to inactivate. *Trends in Neurosciences* **16**, 455–460.

ZILBERTER, Y., MOTIN, L., SOKOLOVA, S., PAPIN, A. & KHODOROV, B. (1991). Ca-sensitive slow inactivation and lidocaine-induced block of sodium channels in rat cardiac cells. *Journal of Molecular and Cellular Cardiology* **23**, suppl. 1, 61–72.

Acknowledgements

This work was supported by grants from the US–Israel Binational Science Foundation (91-256), and the DFG (SFB 194/B3).

Received 5 September 1995; accepted 15 December 1995.